# AN2852
# Application note

## EVL6591-90WADP: 90 W AC-DC asymmetrical half-bridge adapter using L6591 and L6563

## Introduction

This document describes the characteristics and performance of a 90 W wide range input AC-DC adapter based on asymmetrical half-bridge topology (AHB).

The converter comprises a two-stage approach: a PFC front-end stage using the L6563 TM PFC controller and a DC-DC stage that implements the asymmetrical half-bridge (AHB) topology driven by the L6591, the new PWM controller dedicated to this architecture.

Thanks to the AHB topology, the system offers good electrical performance (EPA 2.0 compliant) with a low-voltage and high-current output (12 V - 7.5 A).

The order code for this demonstration board is EVL6591-90WADP.

**Figure 1. EVL6591-90WADP demonstration board**

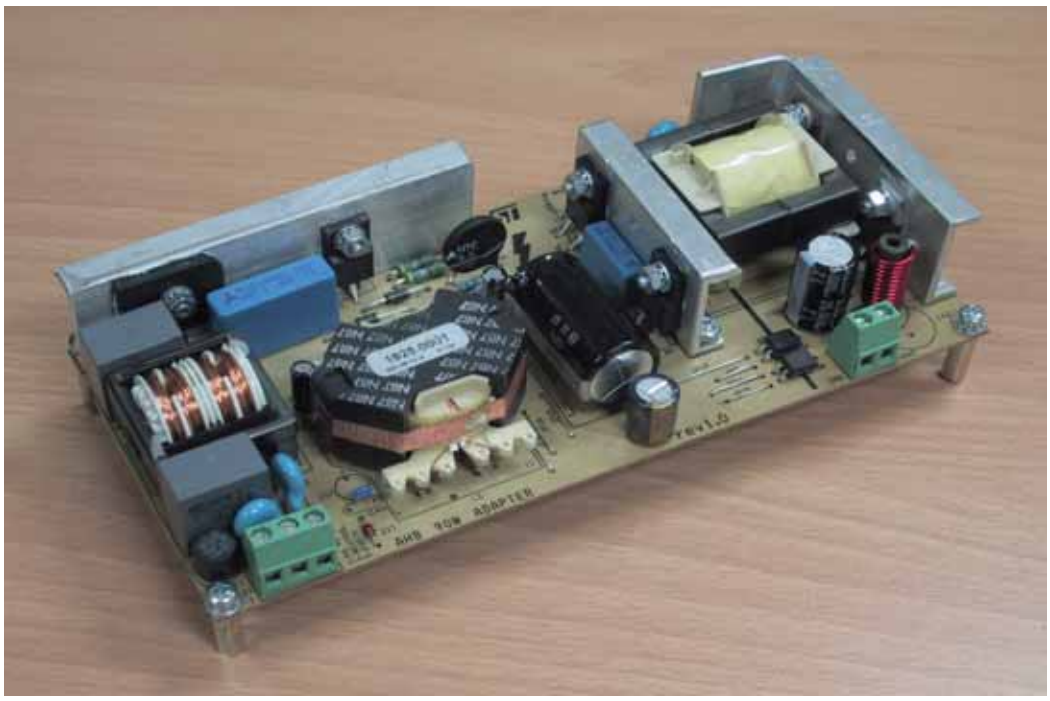

AM01816v1

# Contents

# List of figures

# 1 Main characteristics and circuit description

The main characteristics of the SMPS adapter are as follows:

- Input mains range
  - Vin: 88 ~ 264 Vrms
  - f: 45 ~ 66 Hz
- Output: 12Vdc ± 2% - 7.5 A
- No-load: Pin below 0.35 W
- Protections
  - Short-circuit
  - Overload
  - Ouput overvoltage
  - Brownout
- PCB type and size
  - CEM-1
  - Single-side 70 µm
  - 174 x 78 mm
- Safety: according to EN60065
- EMI: according to EN50022 - class B

The adapter implements a two-stage solution. The front-end PFC uses a boost topology working in transition mode (TM). The IC used is the L6563, advanced TM PFC controller, which integrates all the functions and protection needed to control the stage and an interface with the downstream DC-DC converter.

The power stage of the PFC comprises inductor L2, MOSFET Q1, diode D4 and capacitor C9. The PFC circuit is quite standard and already well described in previous ST application notes. Therefore this note will focus on the AHB stage and its controller, the L6591. This DC-DC converter comprises a half-bridge (MOSFET Q3 and Q4) connected to the output voltage of the PFC stage that drives the series connection of a DC blocking capacitor (C44) and the primary of the transformer (T1). The transformer has two secondary windings with a center tap connection tied to ground. The other ends are connected to the output diodes D12 and D13. The output inductor is between the common cathode of diodes D12 and D13 and the output. The L6591 includes a current mode PWM controller (fixed-frequency solution), gate drivers for both low and high-side MOSFETs with integrated bootstrap diode and all the functions and protections tailored for this topology. The device is housed in an SO-16 narrow package.

This adapter uses the magnetizing current and the output inductor current ripple to obtain the correct primary current direction to achieve zero-voltage switching (ZVS) at turn-on of both MOSFETs. The transformer construction is quite simple as it is a layer type with the primary winding split in two parts (sandwich configuration) and two secondary windings. The primary leakage inductance is about 3% of the magnetizing inductance. The half-bridge is operated at fixed frequency with complementary duty cycles on the two MOSFETs. The high-side FET is on during the D time and the low-side FET is on for the 1-D time. C44 is calculated in order to have a resonance frequency due to Lm and C44 well below the switching frequency (that, in this application, has been set at about 100 kHz). In this way the voltage on C44 is nearly constant and equal to Vin x D where Vin is the high-voltage input

bus and D is the duty cycle. For stability reasons related to the topology, the IC limits the maximum duty cycle at 50%. The current in the primary tank circuit is read by the controller thanks to the sense resistors R81 and R82. The self supply is basically obtained thanks to an auxiliary winding on the AHB transformer. A small charge pump on the auxiliary windings of the PFC inductor helps during the startup phase. A pin dedicated to startup sequencing, a spare latched protection (dedicated here to output overvoltage protection), the soft-start function, the overload protection, an interface with the PFC controller and the integrated high-voltage startup generator complete the features of the L6591. All the functions and protections are detailed in the following sections.

**Figure 2. EVL6591-90WADP schematic**

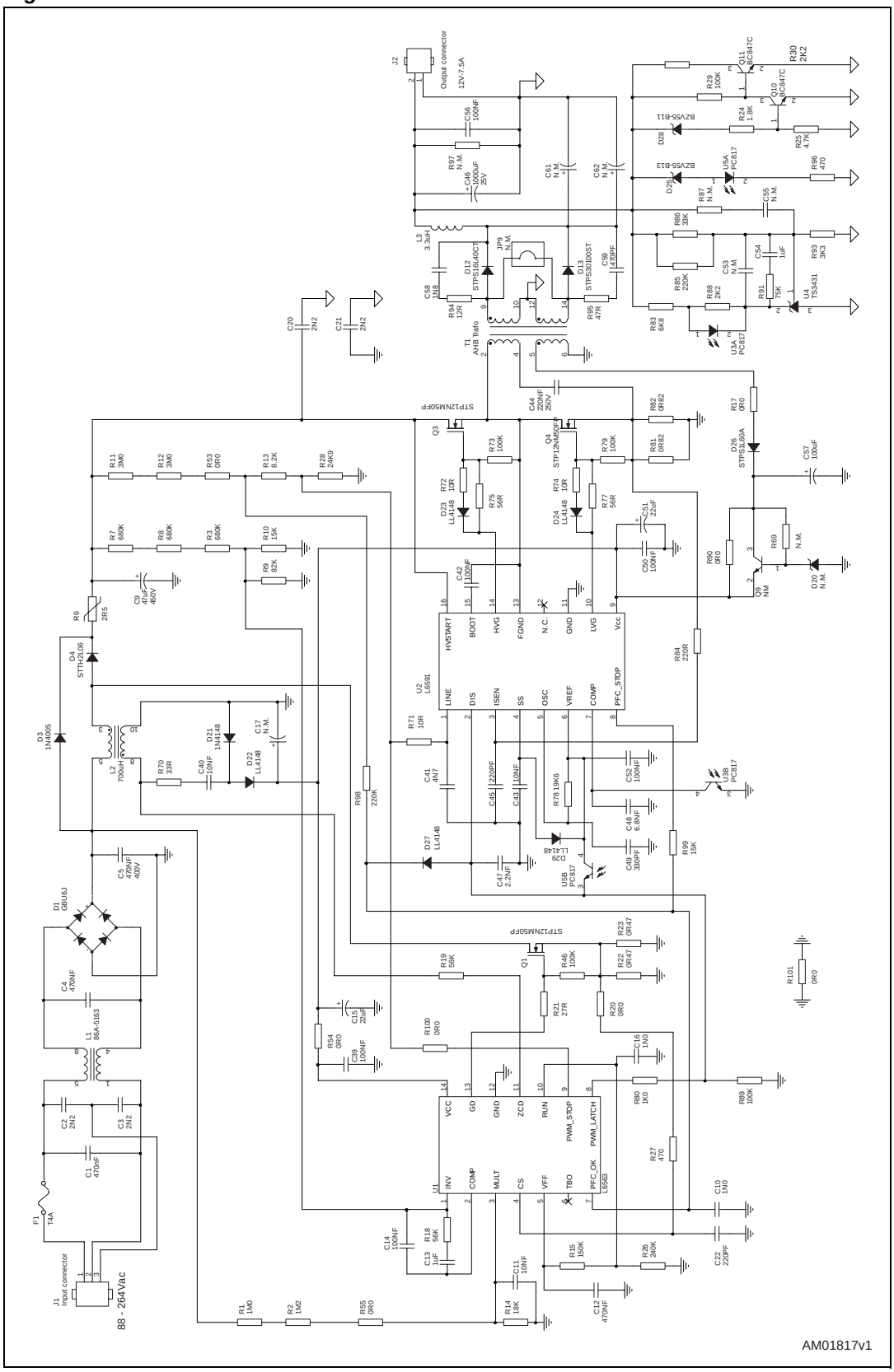

# 2 Operating waveforms

## 2.1 Asymmetrical half-bridge (AHB) typical waveforms

As mentioned before, this application note focuses on the AHB stage. This DC-DC converter has the 400 V PFC bus as input and delivers 12 V at the output.

In *Figure 3* the primary side key waveforms with full load applied are shown. *Figure 4* shows the detail of the two transitions during one switching cycle. When the LVG signal goes down, the current is negative and so the half-bridge node (that has a certain capacitance value due to the Coss of the MOSFETs and the stray capacitance of the circuit) is charged up to 400 V. After the deadtime has elapsed the high-side driver is turned on with zero volts across the high-side MOSFET drain-source pins. The driver activation is visible on the HVG signal when there is the small voltage step on the high part of the waveform.

When the high-side driver is turned off, the primary current is positive, so the half-bridge node is discharged down to zero volts and the body diode of Q4 is activated. After the deadtime the LVG turns on in ZVS condition.

**Figure 3. AHB primary side key waveforms at full load**

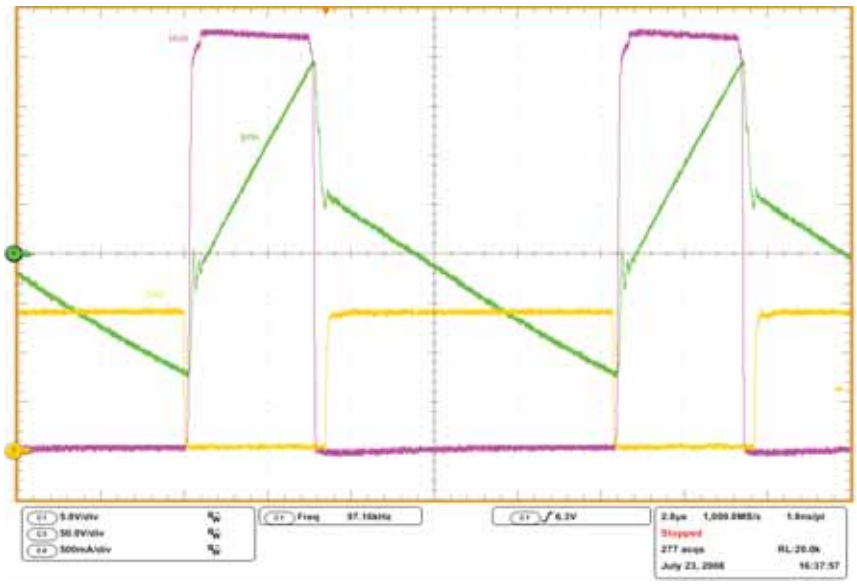

Ch1: LVG pin voltage (yellow)
Ch3: HVG pin voltage (purple)
Ch4: primary winding current (green)

AM01818v1

Typically, in the AHB topology, the most critical transition is the one between LVG turn-off and HVG turn-on. In fact it is visible that the current available to move the half-bridge point is less with respect to the other transition. This is due to the magnetizing current that is not symmetrical with an average value of zero amps but has a certain offset due to the asymmetrical driving of the tank circuit.

The fast current variation during transitions is due to the reversal of the current direction in the secondary windings. The effort in this design was to maintain a negative current after

the positive variation at LVG turn-off. This was done by a correct design of the magnetizing current, output inductor current ripple and choice of turns ratio.

**Figure 4. Detailed AHB zero-voltage switching at full load**

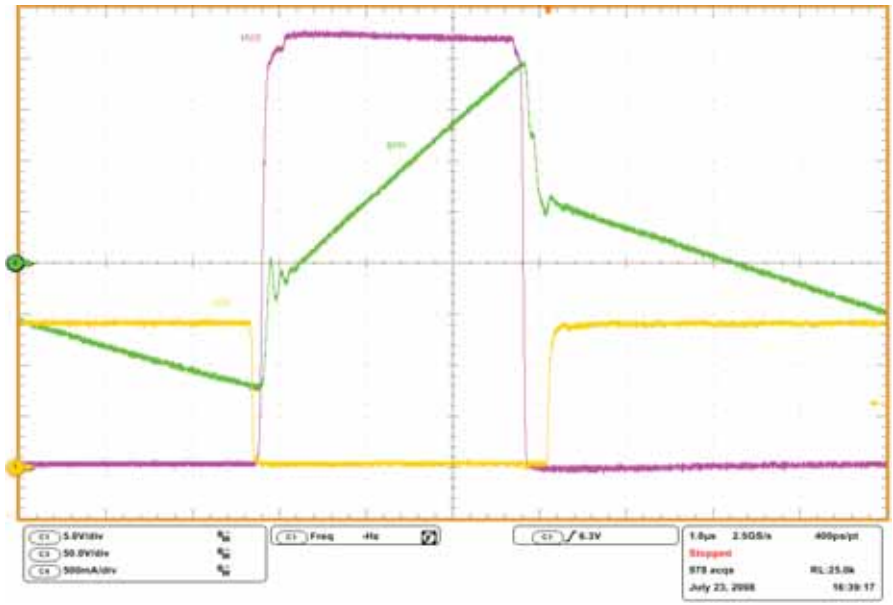

Ch1: LVG pin voltage (yellow)
Ch3: HVG pin voltage (purple)
Ch4: primary winding current (green)

AM01819v1

The ZVS condition is harder to meet as the load increases, so full load is the worst condition to have for a correct ZVS operation. In *Figure 5* the same waveforms are shown with half load. Since the output current is reduced, the fast primary side current variations are also reduced and so the magnetizing current (that remains basically the same if the load changes) becomes proportionally higher. The result is that there is more current available for moving the half-bridge node.

**Figure 5. Detailed AHB zero-voltage switching at half load**

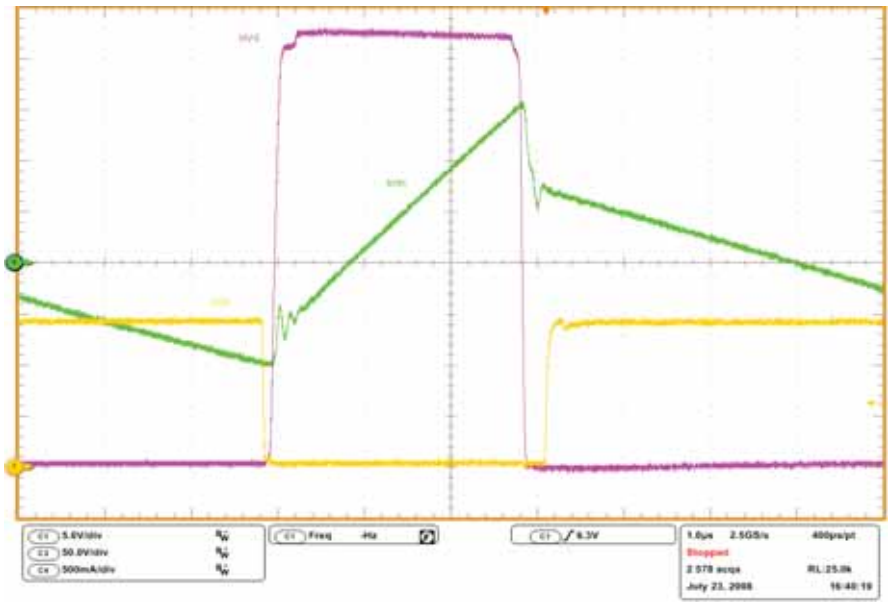

Ch1: LVG pin voltage (yellow)
Ch3: HVG pin voltage (purple)
Ch4: primary winding current (green)

AM01820v1

The key waveforms at the secondary side are shown in *Figure 6*. It is interesting to note that, while the current is swapped between the two diodes, the voltage at their cathode is nearly zero.

**Figure 6. AHB secondary side key waveforms at full load**

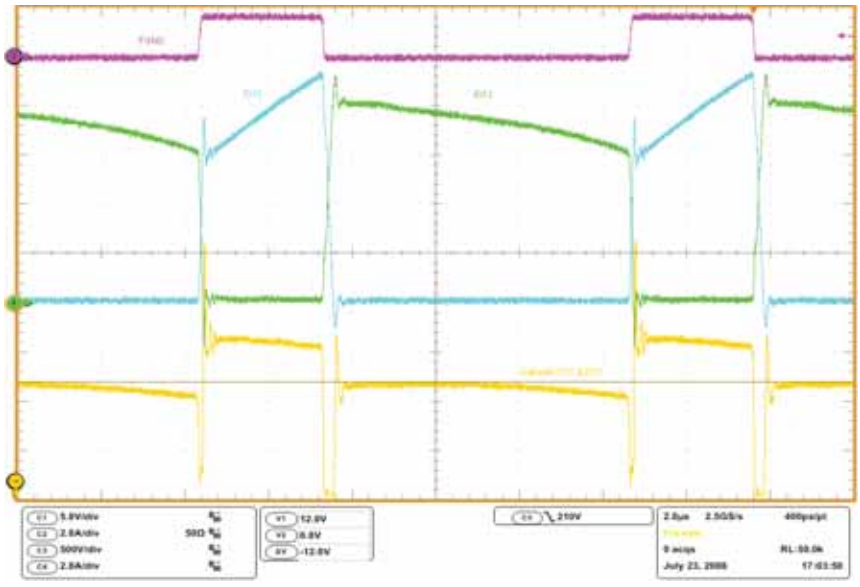

Ch1: D12 and D13 common cathode voltage (yellow)
Ch2: diode D12 current (blue)
Ch3: FGND pin voltage (purple)
Ch4: diode D13 current (green)

AM01821v1

Another peculiarity of this topology is that, since it is asymmetrical, the diode D13 has to carry higher average and RMS current and sustain higher reverse voltage with respect to diode D12. This implies that D13 dissipates a lot more than D12 and makes sense, in order to improve efficiency and save money, to have a synchronous rectification only on D13.

## 2.2 Low-load operation

At light loads (and no-load) conditions the system enters a controlled burst mode operation, allowing input power reduction. The burst mode is activated according to the COMP pin level.

In *Figure 7* and *Figure 8* the burst mode operation with no load is shown. Under a certain load also the PFC stage works in burst mode operation (specifically the PFC enters in burst mode for a load value higher than the one for the AHB). Using the PFC_STOP pin of the L6591 and the PFC_OK pin of the L6563, a simple interface is built in order to keep the burst modes of the two ICs synchronized. This operation allows fast response to a heavy load transition since the PFC is already on when the power is needed. This avoids output voltage dips. The load transition from 0 to 100% and vice versa can be seen in *Figure 9*.

**Figure 7. Burst mode at no load**

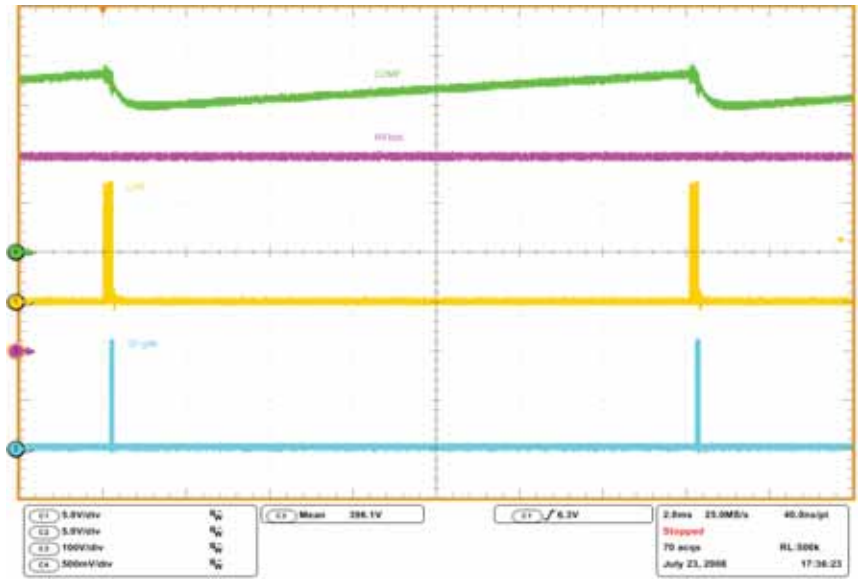

Ch1: LVG pin voltage (yellow)
Ch2: Q1 (PFC MOSFET) gate (blue)
Ch3:PFC output voltage
Ch4: COMP pin voltage (green)

AM01822v1

**Figure 8. Detailed burst mode at no load**

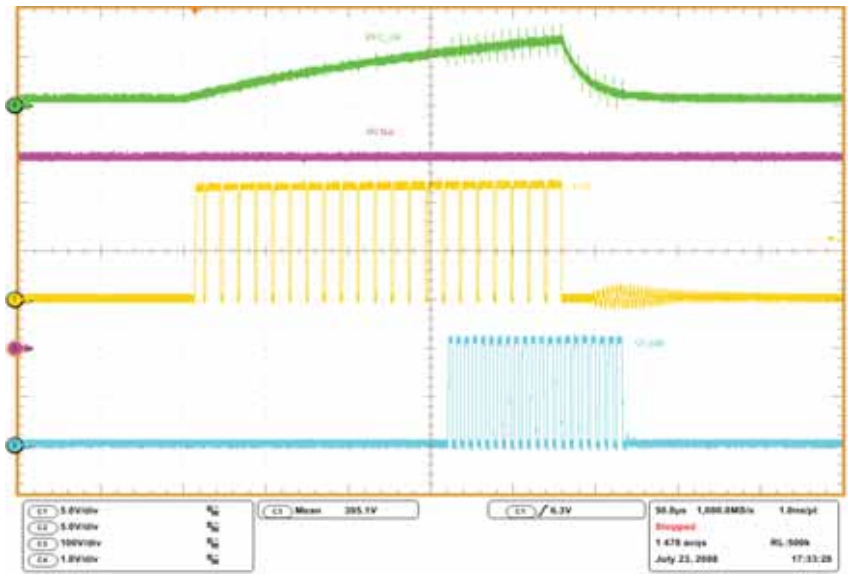

Ch1: LVG pin voltage (yellow)
Ch2: Q1 (PFC MOSFET) gate (blue)
Ch3:PFC output voltage
Ch4: L6563 PFC_OK pin voltage (green)

AM01823v1

**Figure 9. Load transitions**

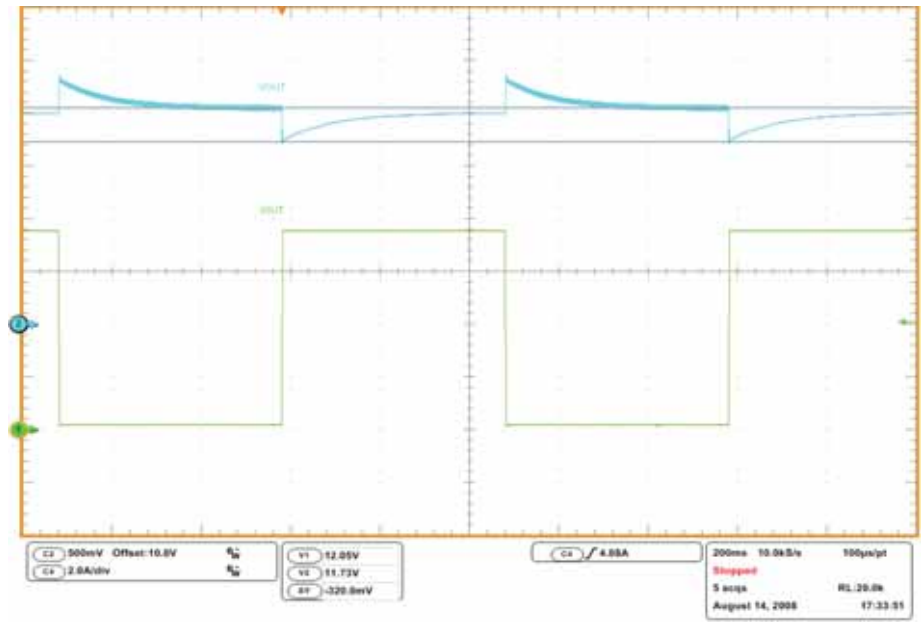

Ch2: output voltage (blue)
Ch4: output current (green)

AM01824v1

## 2.3 Short-circuit protection

A short-circuit at the output activates the overload protection (OLP). *Figure 10* shows the pins involved in this function. When the short-circuit is applied, the COMP pin saturates high. The IC detects this condition and starts charging the SS capacitor. When the SS voltage reaches 5 V, the system shuts down. Diode D29 allows the SS voltage to be clamped at about 5.4 V and the protection has an auto-restart behavior. If the short circuit is not removed, the IC enters the HICCUP mode (*Figure 11*). When the IC is stopped by the OLP, the high-voltage startup generator is invoked only when Vcc falls to 5 V ($V_{CCrestart}$). Thanks to this approach, the period between two restart trials is quite long which reduces the stress on power components.

**Figure 10. Detailed short-circuit behavior**

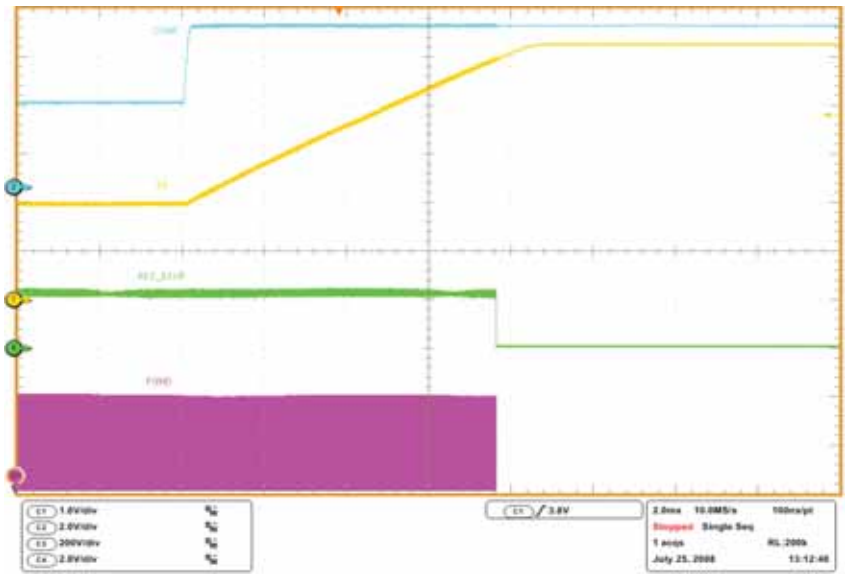

Ch1: SS pin voltage (yellow)
Ch2: COMP pin voltage (blue)
Ch3: FGND pin voltage (purple)
Ch4: PFC_STOP pin voltage (green)

AM01825v1

**Figure 11. HICCUP mode**

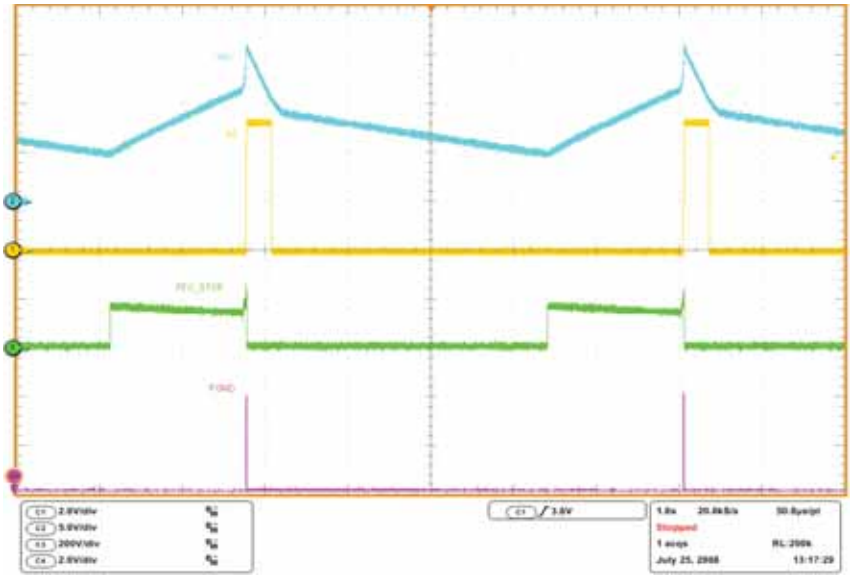

Ch1: SS pin voltage (yellow)
Ch2: COMP pin voltage (blue)
Ch3: FGND pin voltage (purple)
Ch4: PFC_STOP pin voltage (green)

AM01826v1

## 2.4 Overvoltage protection

Since it is impossible to sense the output voltage from the primary side in all load conditions, the OVP senses such voltage directly on the output. A Zener diode (D25) is used as the threshold to activate the protection. The information is passed to the controller using optocoupler U5 that increases the disable pin voltage over the intervention threshold of 4.5 V. In *Figure 12* a loop failure is simulated by shorting R93. The overvoltage protection is invoked and the output voltage reaches a maximum voltage of 14.8 V.

Since this protection uses the disable pin, it is latched. Hence, after PWM is stopped, the HV generator is invoked to keep Vcc voltage between 14 V and 13.5 V. Diode D27 brings the PFC_OK pin voltage over 2.5 V, so the L6563 is also shut down and its consumption goes almost to the startup level. The PWM_LATCH goes high which also keeps the disable pin high. The latched operation is shown in *Figure 13*.

**Figure 12. Detailed OVP intervention**

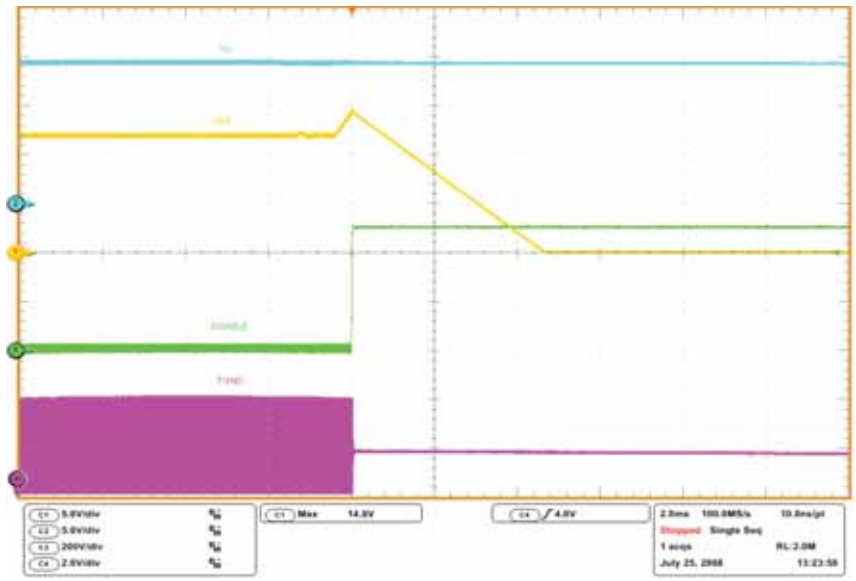

Ch1: output voltage (yellow)
Ch2: Vcc pin voltage (blue)
Ch3: FGND pin voltage (purple)
Ch4: DISABLE pin voltage (green)

AM01827v1

**Figure 13. OVP intervention: system is latched**

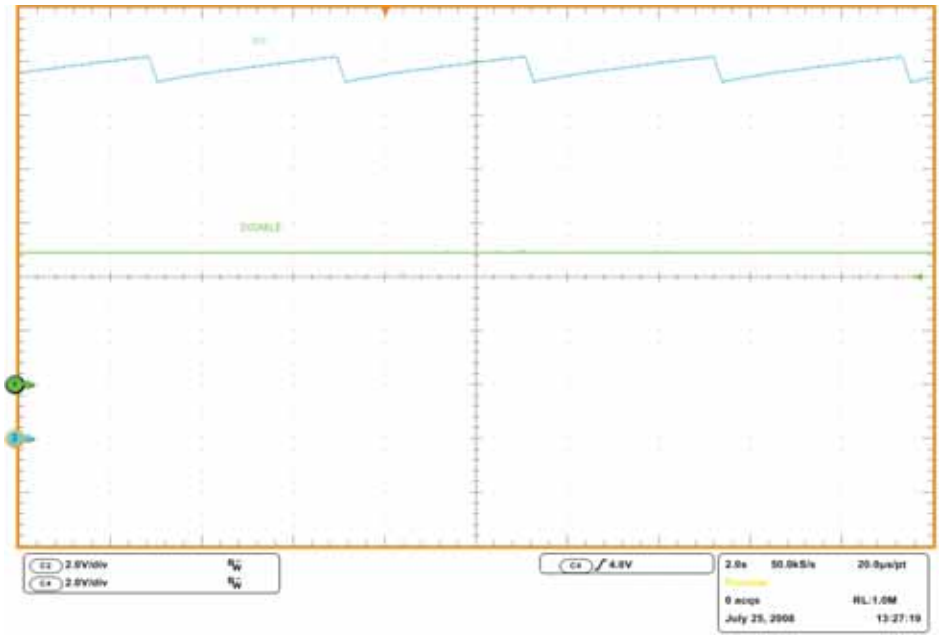

Ch2: Vcc pin voltage (blue)
Ch4: DISABLE pin voltage (green)

AM01828v1

## 2.5 Startup sequence

In this converter the startup sequence is quite particular and merits a detailed explanation.

When the mains is plugged in, the rectified input voltage is present on bulk capacitor C9. Since this value is greater than 80 V, the HV startup generator of the L6591 is turned on and Vcc capacitors are charged with a constant current of about 0.75 mA. This charge time is therefore independent of input voltage level. The L6563 has a turn-on threshold lower than that of L6591, so the PFC controller starts first. The HV startup current is insufficient to power the L6563, so a small charge pump (R70, C40, D21 and D22) is connected to the PFC inductor auxiliary winding. With this circuit, when the L6563 starts, both Vcc voltage and PFC output voltage increase.

Once Vcc > 14 V and line pin voltage is greater than 1.25 V, the L6591 also turns on. At this point the charge pump is insufficient to sustain Vcc current of both ICs and so an auxiliary winding on the AHB transformer is used to provide, together with the charge pump, the power requested by the devices. The complete sequence is shown in *Figure 14*, while the details of the turn-on of both ICs are shown in *Figure 15*. Both figures show the startup at 115Vac mains input. The startup at 230Vac is very similar, the only difference is that the Vcc voltage during steady state operation is a little higher since the charge pump delivers more current.

**Figure 14. Complete startup sequence at 115Vac and full load**

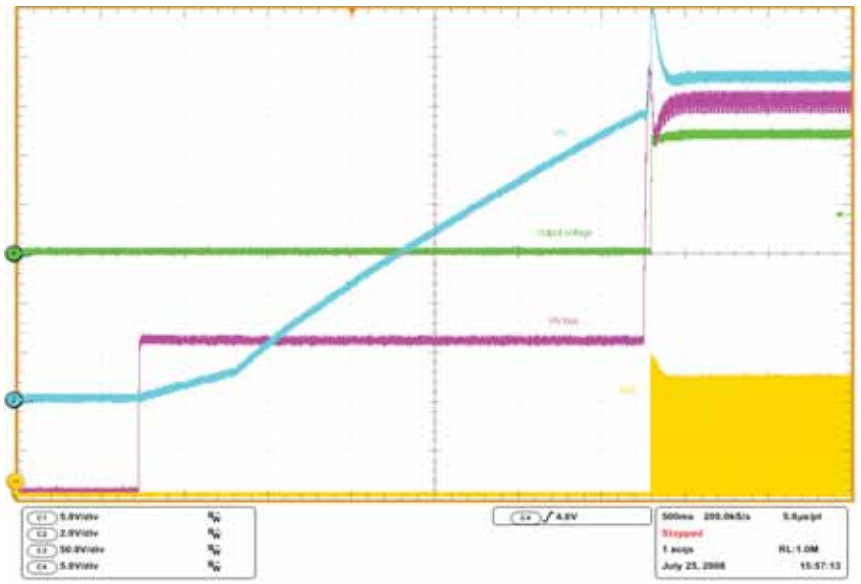

Ch1: LVG voltage (yellow)
Ch2: Vcc pin voltage (blue)
Ch3: PFC output voltage (purple)
Ch4: output voltage (green)

AM01829v1

**Figure 15. Detailed startup sequence at 115Vac and full load**

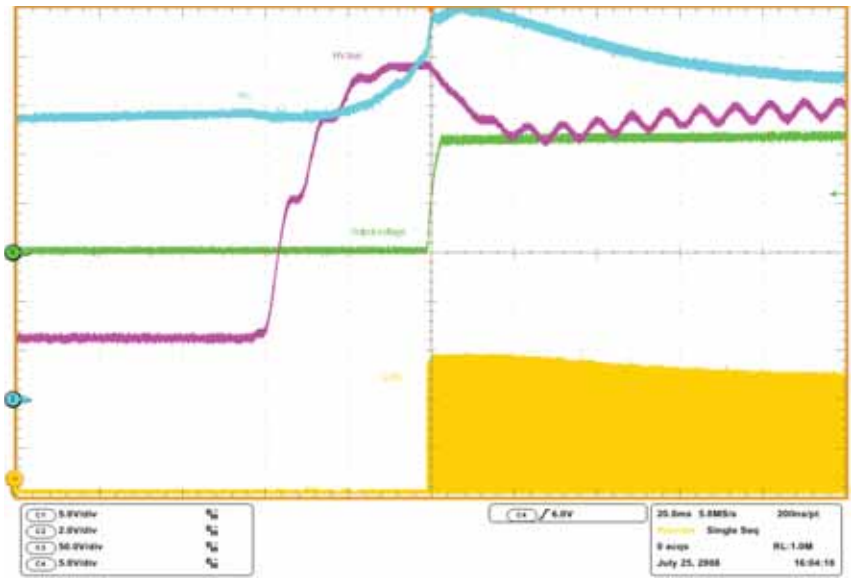

Ch1: LVG voltage (yellow)
Ch2: Vcc pin voltage (blue)
Ch3: PFC output voltage (purple)
Ch4: output voltage (green)

AM01830v1

# 3 Electrical performance

## 3.1 Efficiency measurement and no-load consumption

*Table 1* and *2* give the efficiency measurements taken at the two nominal voltages.

**Table 1. Efficiency at 115Vrms**

| Load [%] | Iout [A] | Vout [V] | Pout [W] | Pin [W] | Eff [%] |
|---|---|---|---|---|---|
| 5% | 0.3746 | 12.12 | 4.54 | 6.80 | 66.77% |
| 10% | 0.7507 | 12.11 | 9.09 | 12.10 | 75.13% |
| 20% | 1.5037 | 12.10 | 18.19 | 21.98 | 82.78% |
| 25% | 1.8787 | 12.09 | 22.71 | 26.83 | 84.66% |
| 40% | 3.0037 | 12.09 | 36.31 | 41.49 | 87.53% |
| 50% | 3.7537 | 12.08 | 45.34 | 51.41 | 88.20% |
| 60% | 4.5037 | 12.08 | 54.40 | 61.44 | 88.55% |
| 75% | 5.6287 | 12.07 | 67.94 | 76.67 | 88.61% |
| 80% | 6.0037 | 12.07 | 72.46 | 81.77 | 88.62% |
| 100% | 7.5037 | 12.06 | 90.49 | 102.48 | 88.30% |

**Table 2. Efficiency at 230Vrms**

| Load [%] | Iout [A] | Vout [V] | Pout [W] | Pin [W] | Eff [%] |
|---|---|---|---|---|---|
| 5% | 0.3746 | 12.12 | 4.54 | 6.58 | 68.97% |
| 10% | 0.7507 | 12.11 | 9.09 | 12.41 | 73.26% |
| 20% | 1.5037 | 12.10 | 18.19 | 22.30 | 81.59% |
| 25% | 1.8787 | 12.09 | 22.71 | 27.02 | 84.06% |
| 40% | 3.0037 | 12.08 | 36.28 | 41.37 | 87.71% |
| 50% | 3.7537 | 12.08 | 45.34 | 51.05 | 88.82% |
| 60% | 4.5037 | 12.07 | 54.36 | 60.83 | 89.36% |
| 75% | 5.6287 | 12.07 | 67.94 | 75.60 | 89.87% |
| 80% | 6.0037 | 12.07 | 72.46 | 80.56 | 89.95% |
| 100% | 7.5037 | 12.06 | 90.49 | 100.55 | 90.00% |

The efficiency taken at 25%, 50%, 75% and 100% of rated load allows calculating the average efficiency required by the ENERGY STAR® specification.

**Table 3. Average efficiency for EPA**

| Vin [Vrms] | Average efficiency for EPA |
|---|---|
| 115 | 87.44% |
| 230 | 88.19% |

*Table 4* shows the no-load consumption. The adapter has good values (about 300 mW at 230Vac), considering that it is a two-stage system with the PFC stage always on.

**Table 4. No-load consumption**

| Vin [Vac] | 90 | 115 | 135 | 180 | 230 | 264 |
|---|---|---|---|---|---|---|
| Pin [W] | 0.215 | 0.225 | 0.235 | 0.255 | 0.290 | 0.315 |

This adapter meets the two conditions required by ENERGY STAR® specification version 2.0 (average efficiency > 87% and no-load input power < 0.5 W) for an external power supply (EPS). Therefore this SMPS is EPA 2.0 compliant.

*Figure 16* shows the graph of the efficiency vs. output power while *Figure 17* shows the graph of the input power vs. input voltage with no load applied.

**Figure 16. Efficiency vs. O/P power**

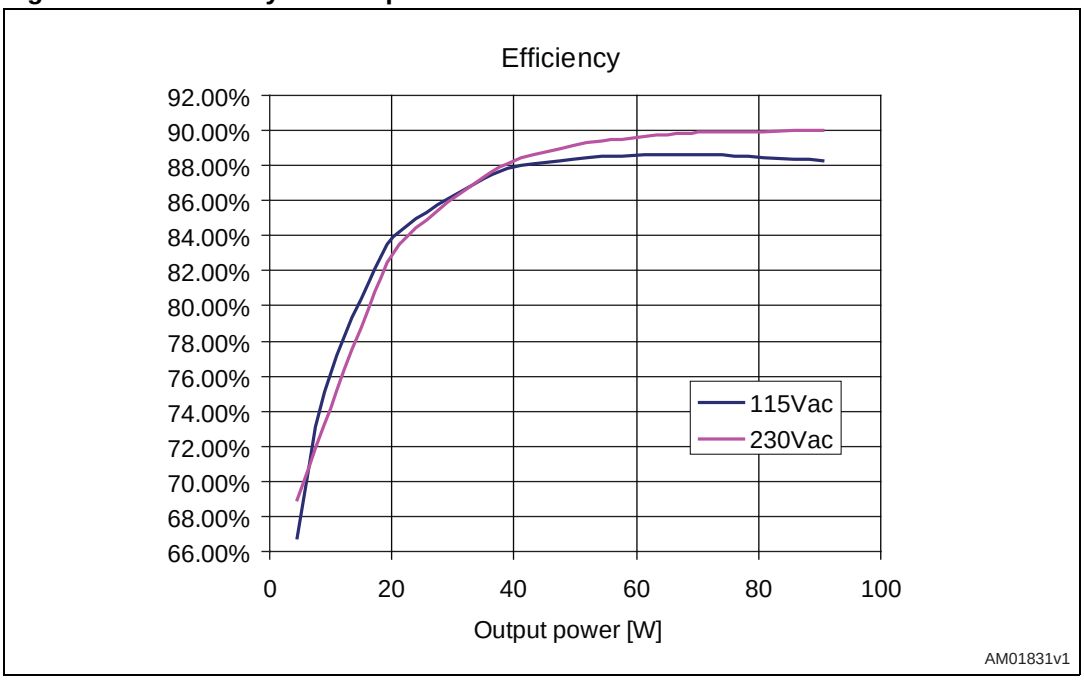

**Figure 17. No-load consumption**

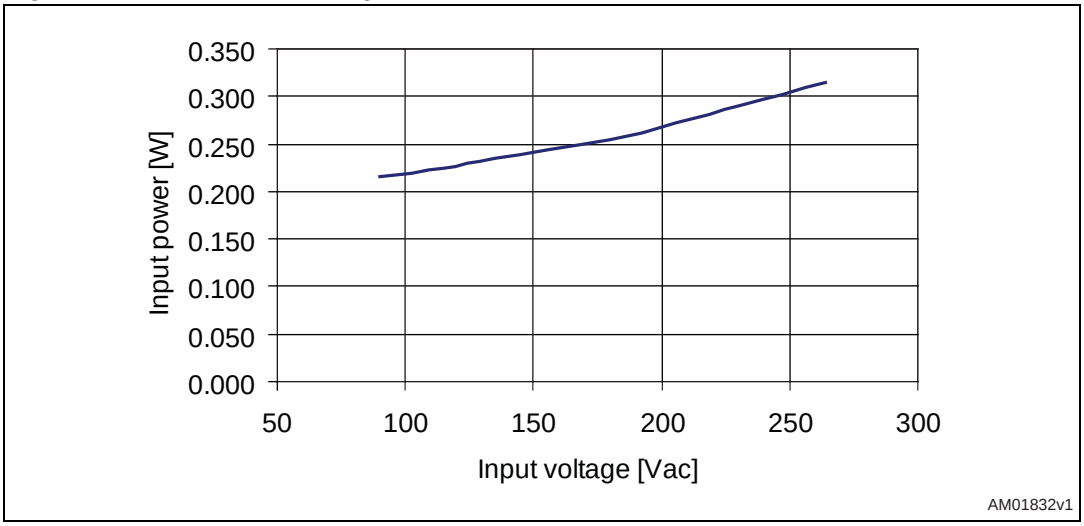


Some measurements with low output loads were also taken, refer to *Table 5* and *Table 6*.

**Table 5. Low-load efficiency at 115Vrms**

| Pout [W] | Iout [mA] | Vout [V] | Pin [W] | Eff [%] |
|---|---|---|---|---|
| 1.50 | 124.50 | 12.12 | 2.696 | 55.97% |
| 1.00 | 82.50 | 12.12 | 1.883 | 53.10% |
| 0.50 | 42.02 | 12.12 | 1.076 | 47.31% |
| 0.25 | 21.05 | 12.11 | 0.654 | 38.98% |

**Table 6. Low-load efficiency at 230Vrms**

| Pout [W] | Iout [mA] | Vout [V] | Pin [W] | Eff [%] |
|---|---|---|---|---|
| 1.50 | 124.50 | 12.12 | 2.598 | 58.08% |
| 1.00 | 82.50 | 12.12 | 1.802 | 55.49% |
| 0.50 | 42.02 | 12.12 | 1.087 | 46.83% |
| 0.25 | 21.05 | 12.11 | 0.704 | 36.21% |

## 3.2 Harmonic content measurement

The front-end PFC stage provides the reduction of the mains harmonic, allowing meeting European EN61000-3-2 and Japanese JEIDA-MITI standards for class D equipment. *Figure 18* and *19* show the harmonic contents of the mains current at full load.

A measure has been done also with 75 W input power which is the lower limit for using harmonic reduction techniques.

**Figure 18. EN61000-3-2 measurements at full load**

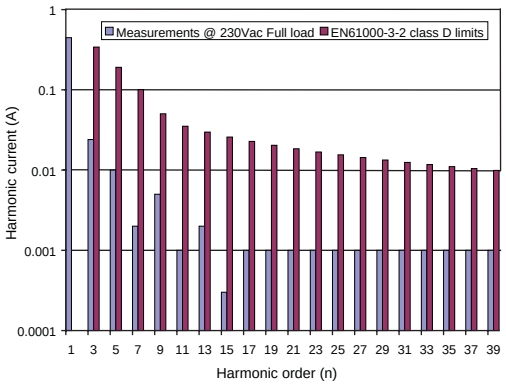


**Figure 19. JEIDA-MITI measurements at full load**

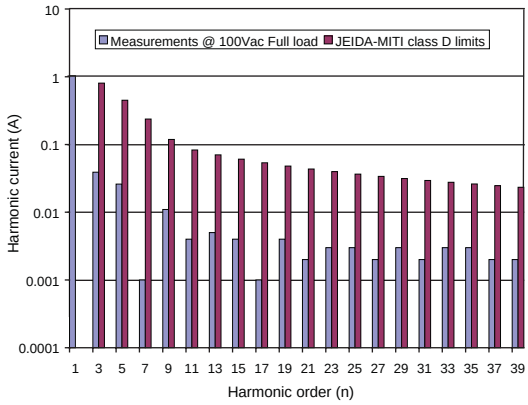


**Figure 20. EN61000-3-2 measurements at 75 W input**

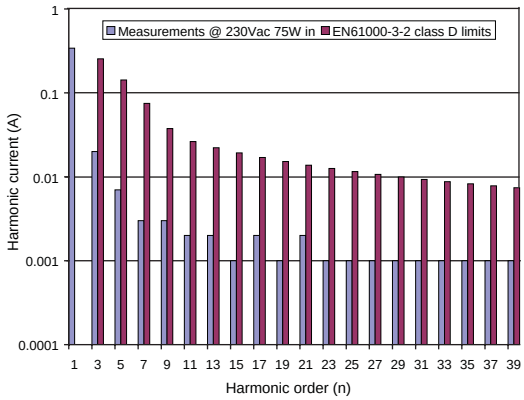


**Figure 21. JEIDA-MITI measurements at 75 W input**

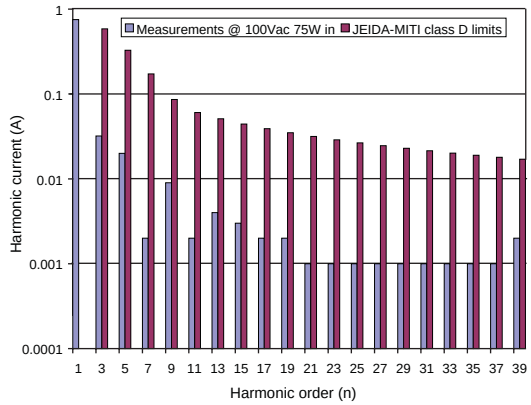

To evaluate the performance of the PFC stage also, the PF and THD vs. input voltage graphs are shown in *Figure 22* and *23* at full load and 75 W input power.

**Figure 22. PF vs. input voltage**

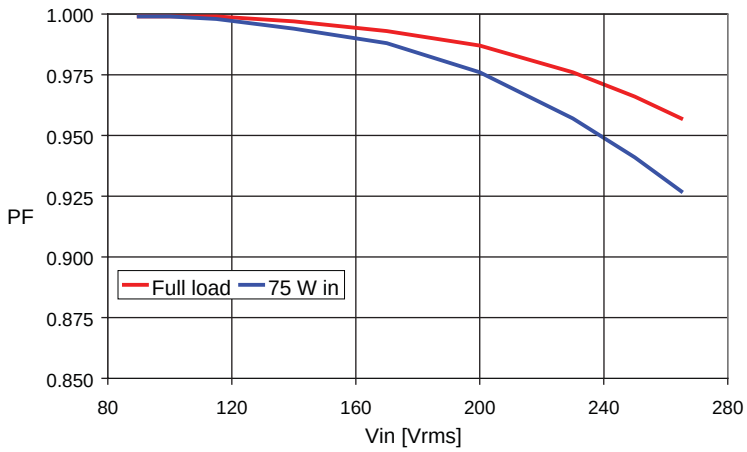


**Figure 23. THD vs. input voltage**

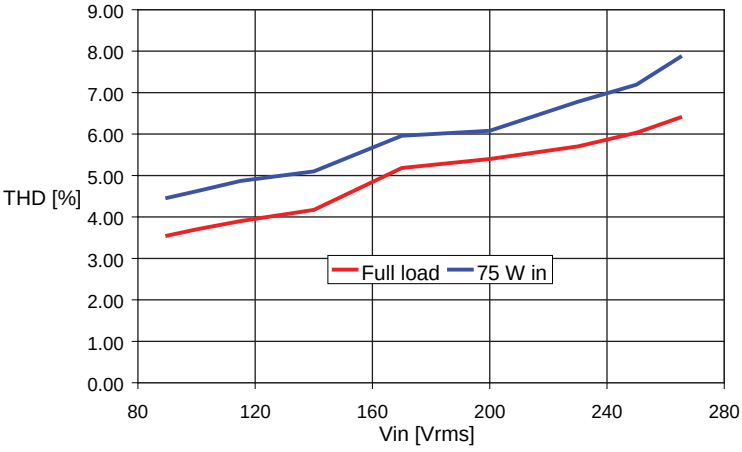

# 4 Thermal measurements

A thermal analysis of the board was performed using an IR camera, refer to *Figure 24* and *25*.

**Figure 24. Thermal map at 115Vac - full load**

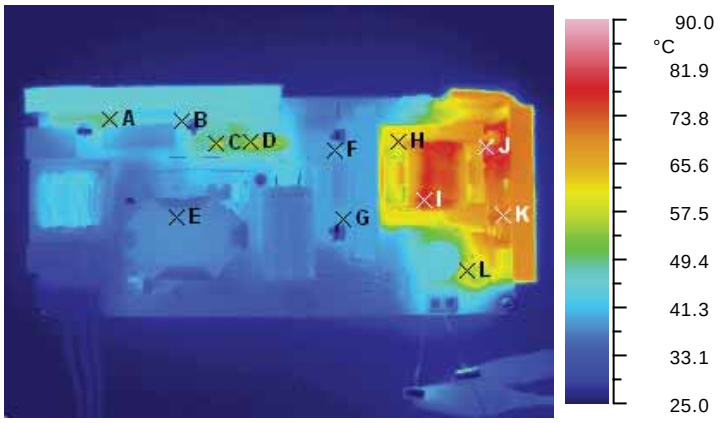


**Figure 25. Thermal map at 230Vac - full load**

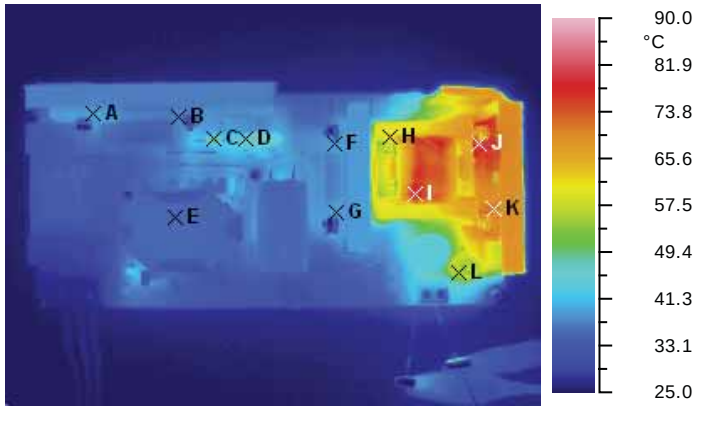


**Table 7. Temperature of key components ($T_{amb}$ = 25 °C, emissivity = 0.95 for all points)**

| Point | Reference | T [°C] at 115Vac | T [°C] at 230Vac |
|---|---|---|---|
| A | D1 (Input bridge) | 49.5 | 39.5 |
| B | Q1 (PFC MOSFET) | 46.4 | 37.9 |
| C | D4 (PFC diode) | 56.8 | 49.1 |
| D | R6 (NTC) | 55.9 | 47.1 |
| E | L2 (PFC coil) | 38.1 | 35.7 |
| F | Q4 (AHB low-side MOSFET) | 43.8 | 39.2 |

**Table 7. Temperature of key components ($T_{amb}$ = 25 °C, emissivity = 0.95 for all points) (continued)**

| Point | Reference | T [°C] at 115Vac | T [°C] at 230Vac |
|---|---|---|---|
| G | Q3 (AHB high side MOSFET) | 40.2 | 39.3 |
| H | T1 (AHB transformer ferrite) | 64.8 | 63.4 |
| I | T1 (AHB transformer winding) | 81.2 | 80.1 |
| J | D13 (AHB output diode) | 83.1 | 81.8 |
| K | D12 (AHB output diode) | 73.7 | 72.8 |
| L | L3 (Output inductor) | 58.7 | 57.9 |

# 5 Conducted noise measurements (pre-compliance test)

*Figure 26* and *27* show the conducted noise measurements performed at the two nominal voltages with peak detection and considering only the worst phase. Both measures are well below the average limit (taken from EN55022 CLASS B norm).

**Figure 26. CE peak measure at 115Vac and full load**

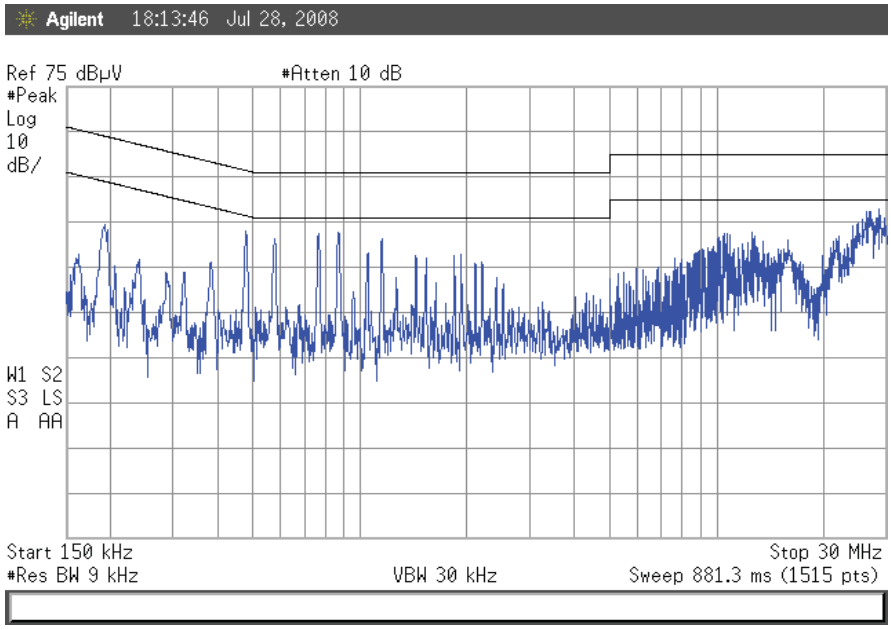


**Figure 27. CE peak measure at 230Vac and full load**

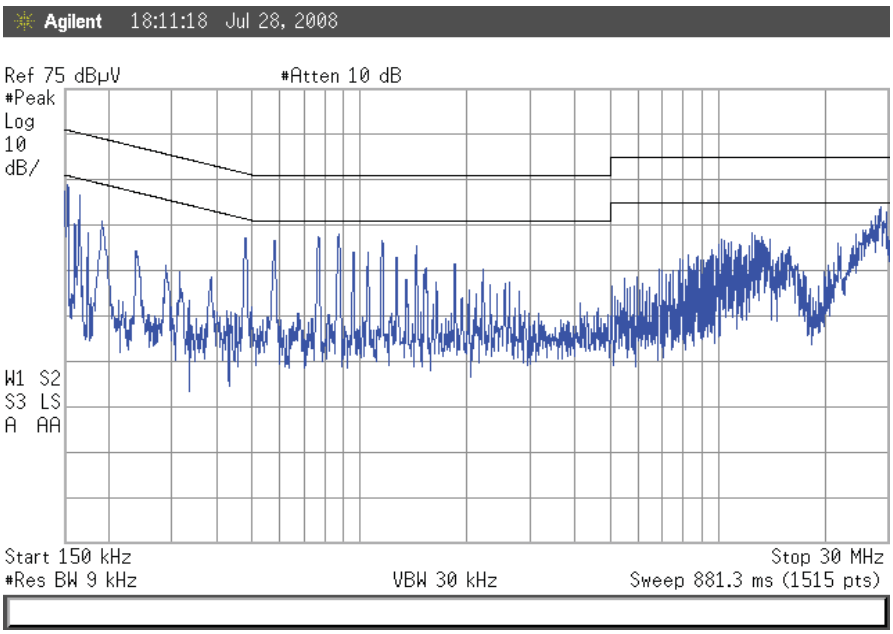

# 6 Bill of material

**Table 8. EVL6591-90WADP bill of materials**

| Ref | Value | Description | Manufacturer |
|---|---|---|---|
| C1 | 470 NF | Polypropylene X2 capacitor - R46 KI 3470--02 M | Arcotronics |
| C10 | 1N0 | SMD ceramic capacitor X7R - 50 V | AVX |
| C11 | 10 NF | SMD ceramic capacitor X7R - 50 V | AVX |
| C12 | 470 NF | SMD ceramic capacitor X7R - 25 V | AVX |
| C13 | 1 µF | SMD ceramic capacitor X7R - 25 V | AVX |
| C14 | 100 NF | SMD ceramic capacitor X7R - 50 V | AVX |
| C15 | 22 µF | Electrolytic capacitor YXF - 50 V | Rubycon |
| C16 | 1N0 | SMD ceramic capacitor X7R - 50 V | AVX |
| C17 | N.M. | Electrolytic capacitor | |
| C2 | 2N2 | Ceramic Y1 capacitor - DE1E3KX222M | Murata |
| C20 | 2N2 | Ceramic Y1 capacitor - DE1E3KX222M | Murata |
| C21 | 2N2 | Ceramic Y1 capacitor - DE1E3KX222M | Murata |
| C22 | 220 PF | SMD ceramic capacitor NP0 - 50 V | AVX |
| C3 | 2N2 | Ceramic Y1 capacitor - DE1E3KX222M | Murata |
| C39 | 100 NF | SMD ceramic capacitor X7R - 50 V | AVX |
| C4 | 470 NF | Polypropylene X2 capacitor - R46 KI 3470--02 M | Arcotronics |
| C40 | 10 NF | Ceramic capacitor X7R - 50 V | AVX |
| C41 | 4N7 | SMD ceramic capacitor X7R - 50 V | AVX |
| C42 | 100 NF | SMD ceramic capacitor X7R - 50 V | AVX |
| C43 | 10 NF | SMD ceramic capacitor X7R - 50 V | AVX |
| C44 | 220 NF | Polypropylene capacitor - B32652A3224J | EPCOS |
| C45 | 220 PF | SMD ceramic capacitor NP0 - 50 V | AVX |
| C46 | 1000 µF | Electrolytic capacitor ZL - 25 V | Rubycon |
| C47 | 2.2 NF | SMD ceramic capacitor X7R - 50 V | AVX |
| C48 | 6.8 NF | SMD ceramic capacitor X7R - 50 V | AVX |
| C49 | 330 PF | SMD ceramic capacitor NP0 - 50 V - 2% | AVX |
| C5 | 470 NF | Polypropylene capacitor - PHE426KD6470JR06L2 | EVOX-RIFA |
| C50 | 100 NF | SMD ceramic capacitor X7R - 50 V | AVX |
| C51 | 22 uF | Electrolytic capacitor YXF - 50 V | Rubycon |
| C52 | 100 NF | SMD ceramic capacitor X7R - 50 V | AVX |
| C53 | N.M. | SMD ceramic capacitor X7R - 50 V | |
| C54 | 1 uF | SMD ceramic capacitor X7R - 25 V | AVX |

**Table 8. EVL6591-90WADP bill of materials (continued)**

| Ref | Value | Description | Manufacturer |
|---|---|---|---|
| C55 | N.M. | SMD ceramic capacitor X7R - 50 V | |
| C56 | 100 NF | SMD ceramic capacitor X7R - 50 V | AVX |
| C57 | 100 µF | Electrolytic capacitor YXF - 35 V | Rubycon |
| C58 | 1N8 | SMD ceramic capacitor X7R - 50 V | AVX |
| C59 | 470 PF | SMD ceramic capacitor X7R - 50 V | AVX |
| C61 | N.M. | Electrolytic capacitor | |
| C62 | N.M. | Electrolytic capacitor | |
| C9 | 47 µF | Electrolytic capacitor - 450 V - EEUED2W470 | Panasonic |
| D1 | GBU6J | Bridge rectifier | Vishay |
| D12 | STPS16L40CT | Power Schottky rectifier | STMicroelectronics |
| D13 | STPS30100ST | Power Schottky rectifier | STMicroelectronics |
| D20 | N.M. | Zener diode | |
| D21 | 1N4148 | Diode | |
| D22 | LL4148 | SMD diode | |
| D23 | LL4148 | SMD diode | |
| D24 | LL4148 | SMD diode | |
| D25 | BZV55-B13 | Zener diode - 2% | Vishay |
| D26 | STPS1L60A | SMD Schottky diode | STMicroelectronics |
| D27 | LL4148 | SMD diode | |
| D28 | BZV55-B11 | Zener diode - 2% | Vishay |
| D29 | LL4148 | SMD diode | |
| D3 | 1N4005 | Diode | Vishay |
| D4 | STTH2L06 | Ultrafast diode | STMicroelectronics |
| F1 | T4 A | PCB fuse TR5 | Wickmann |
| J1 | IN connector | Screw connector - MKDS 1,5/3-5.08 | Phoenix Contact |
| J2 | OUT connector | Screw connector - MKDS 1,5/2-5.08 | Phoenix Contact |
| JP9 | N.M. | Wire jumper | |
| L1 | 2x25 mH | Input EMI filter - HF2826-253Y1R2-T01 | TDK |
| L2 | 700 µH | PFC inductor - 1825.0001 | Magnetica |
| L3 | 3.3 µH | Power inductor - PCV-0-332-10L | Coilcraft |
| Q1 | STP12NM50FP | Power MOSFET | STMicroelectronics |
| Q10 | BC847C | Small signal BJT | |
| Q11 | BC847C | Small signal BJT | |
| Q3 | STP12NM50FP | Power MOSFET | STMicroelectronics |
| Q4 | STP12NM50FP | Power MOSFET | STMicroelectronics |

**Table 8. EVL6591-90WADP bill of materials (continued)**

| Ref | Value | Description | Manufacturer |
|---|---|---|---|
| Q9 | N.M. | Small signal BJT | |
| R1 | 1M0 | SMD film resistor - 5% - 250 ppm/°C - 1206 | Vishay |
| R10 | 15 kΩ | SMD film resistor - 1% - 100 ppm/°C - 0805 | Vishay |
| R100 | 0R0 | SMD film resistor - 1206 | Vishay |
| R101 | 0R0 | SMD film resistor - 1206 | Vishay |
| R11 | 3M0 | Film resistor - 1% - 100 ppm/°C - 0.4W | Vishay |
| R12 | 3M0 | Film resistor - 1% - 100 ppm/°C - 0.4W | Vishay |
| R13 | 8.2 kΩ | SMD film resistor - 1% - 100 ppm/°C - 0805 | Vishay |
| R14 | 18 kΩ | SMD film resistor - 5% - 250 ppm/°C - 1206 | Vishay |
| R15 | 150 kΩ | SMD film resistor - 5% - 250 ppm/°C - 1206 | Vishay |
| R17 | 0R0 | SMD film resistor - 1206 | Vishay |
| R18 | 56 kΩ | SMD film resistor - 5% - 250 ppm/°C - 0805 | Vishay |
| R19 | 56 kΩ | SMD film resistor - 5% - 250 ppm/°C - 0805 | Vishay |
| R2 | 1M2 | SMD film resistor - 5% - 250 ppm/°C - 1206 | Vishay |
| R20 | 0R0 | SMD film resistor - 1206 | Vishay |
| R21 | 27 Ω | SMD film resistor - 5% - 250 ppm/°C - 1206 | Vishay |
| R22 | 0R47 | Film resistor – 5% – 250 ppm/°C - 0.4W | Vishay |
| R23 | 0R47 | Film resistor – 5% – 250 ppm/°C - 0.4W | Vishay |
| R24 | 1.8 kΩ | SMD film resistor - 1% - 100 ppm/°C - 0805 | Vishay |
| R25 | 4.7 kΩ | SMD film resistor - 1% - 100 ppm/°C - 0805 | Vishay |
| R26 | 240 kΩ | SMD film resistor - 5% - 250 ppm/°C - 0805 | Vishay |
| R27 | 470 | SMD film resistor - 5% - 250 ppm/°C - 1206 | Vishay |
| R28 | 24K9 | SMD film resistor - 1% - 100 ppm/°C - 0805 | Vishay |
| R29 | 100 kΩ | SMD film resistor - 5% - 250 ppm/°C - 0805 | Vishay |
| R3 | 680 kΩ | Film resistor - 1% - 100 ppm/°C - 1206 | Vishay |
| R30 | 2K2 | SMD film resistor - 1% - 100 ppm/°C - 1206 | Vishay |
| R46 | 100 kΩ | SMD film resistor - 5% - 250 ppm/°C - 0805 | Vishay |
| R53 | 0R0 | SMD film resistor - 1206 | Vishay |
| R54 | 0R0 | SMD film resistor - 1206 | Vishay |
| R55 | 0R0 | SMD film resistor - 1206 | Vishay |
| R6 | 2R5 | NTC resistor S237 - B57237S0259M000 | EPCOS |
| R69 | N.M. | SMD resistor - 0805 | Vishay |
| R7 | 680 kΩ | Film resistor - 1% - 100 ppm/°C - 0.4 W | Vishay |
| R70 | 33 Ω | SMD film resistor - 5% - 250 ppm/°C - 1206 | Vishay |
| R71 | 10 Ω | SMD film resistor - 5% - 250 ppm/°C - 1206 | Vishay |

**Table 8. EVL6591-90WADP bill of materials (continued)**

| Ref | Value | Description | Manufacturer |
|---|---|---|---|
| R72 | 10 Ω | SMD film resistor - 5% - 250 ppm/°C - 0805 | Vishay |
| R73 | 100 kΩ | SMD film resistor - 5% - 250 ppm/°C - 0805 | Vishay |
| R74 | 10 Ω | SMD film resistor - 5% - 250 ppm/°C - 0805 | Vishay |
| R75 | 56 Ω | SMD film resistor - 5% - 250 ppm/°C - 0805 | Vishay |
| R77 | 56 Ω | SMD film resistor - 5% - 250 ppm/°C - 0805 | Vishay |
| R78 | 19K6 | SMD film resistor - 1% - 100 ppm/°C - 0805 | Vishay |
| R79 | 100 kΩ | SMD film resistor - 5% - 250 ppm/°C - 0805 | Vishay |
| R8 | 680 kΩ | Film resistor - 1% - 100 ppm/°C - 0.4 W | Vishay |
| R80 | 1K0 | SMD film resistor - 5% - 250 ppm/°C - 0805 | Vishay |
| R81 | 0R82 | SMD film resistor - 5% - 250 ppm/°C - 1206 | Vishay |
| R82 | 0R82 | SMD film resistor - 5% - 250 ppm/°C - 1206 | Vishay |
| R83 | 6K8 | SMD film resistor - 5% - 250 ppm/°C - 0805 | Vishay |
| R84 | 220 Ω | SMD film resistor - 5% - 250 ppm/°C - 1206 | Vishay |
| R85 | 220 kΩ | SMD film resistor - 1% - 100 ppm/°C - 0805 | Vishay |
| R86 | 33 kΩ | SMD film resistor - 1% - 100 ppm/°C - 0805 | Vishay |
| R87 | N.M. | SMD resistor - 0805 | Vishay |
| R88 | 2K2 | SMD film resistor - 5% - 250 ppm/°C - 0805 | Vishay |
| R89 | 100 kΩ | SMD film resistor - 5% - 250 ppm/°C - 1206 | Vishay |
| R9 | 82 kΩ | SMD film resistor - 1% - 100 ppm/°C - 0805 | Vishay |
| R90 | 0R0 | SMD film resistor – 0805 | Vishay |
| R91 | 75 kΩ | SMD film resistor - 5% - 250 ppm/°C - 0805 | Vishay |
| R93 | 3K3 | SMD film resistor - 1% - 100 ppm/°C - 0805 | Vishay |
| R94 | 12 Ω | SMD film resistor - 5% - 250 ppm/°C - 1206 | Vishay |
| R95 | 47 Ω | SMD film resistor - 5% - 250 ppm/°C - 1206 | Vishay |
| R96 | 470 | SMD film resistor - 1% - 100 ppm/°C - 1206 | Vishay |
| R97 | N.M. | SMD resistor - 1206 | Vishay |
| R98 | 220 Ω | SMD film resistor - 5% - 250 ppm/°C - 1206 | Vishay |
| R99 | 15 kΩ | SMD film resistor - 5% - 250 ppm/°C - 1206 | Vishay |
| T1 | Transformer | AHB transformer 1754.0004 | Magnetica |
| U1 | L6563 | Advanced TM PFC controller | STMicroelectronics |
| U2 | L6591 | PWM controller for ZVS half-bridge | STMicroelectronics |
| U3 | PC817 | Optocoupler - PC817X1J000F | Sharp |
| U4 | TS3431AILT | SMD voltage reference - 1% | STMicroelectronics |
| U5 | PC817 | Optocoupler - PC817X1J000F | Sharp |

# 7 PFC coil specifications

- Application type: consumer, IT
- Transformer type: open
- Coil former: vertical type, 6+6 pins
- Max. temp. rise: 45°C
- Max. operating ambient temp.: 60°C
- Mains insulation: N.A.

## 7.1 Electrical characteristics

- Converter topology: boost, transition mode
- Core type: RM14 - N87 or equivalent
- Min. operating frequency: 20 kHz
- Primary inductance: 700 µH 10% at 1 kHz - 0.25 V (see *Note 1*)
- Peak primary current: 3.5 $A_{pk}$
- RMS primary current: 1.25 $A_{RMS}$.

*Note: 1 measured between pins 3-5*

**Figure 28. Electrical diagram**

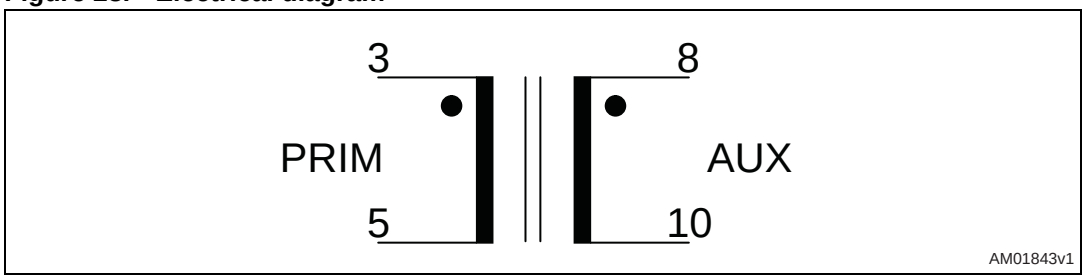


**Table 9. Winding characteristics**

| Pins | Winding | RMS current | Nr. of turns | Wire type |
|---|---|---|---|---|
| 3 – 5 | Primary | 1.25 $A_{RMS}$ | 53 | Stranded 7 x Ø 0.28 mm – G2 |
| 8 – 10 | AUX (1) | 0.05 $A_{RMS}$ | 4 spaced | Ø 0.28 mm – G2 |

1. Auxiliary winding is wound on top of primary winding

## 7.2 Mechanical aspect and pin numbering

- Maximum height from PCB: 22 mm
- Coil former type: vertical, 6+6 pins
- Pin distance: 5.08 mm
- Row distance: 35.56 mm
- Pins removed: # 1, 4, 6, 7, 9, 11, 12
- External copper shield: bare, wound around the ferrite core including the windings and coil former. Height is 7 mm. Connected by a solid wire soldered to pin 10
- Manufacturer: Magnetica
- P/N: 1825.0001.

**Figure 29. Bottom view**

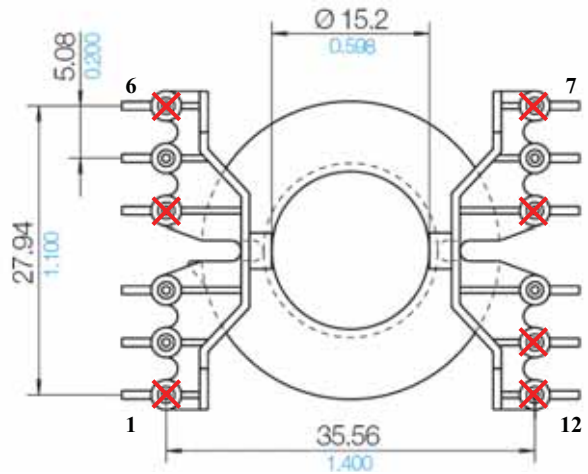

# 8 AHB transformer specifications

- Application type: consumer, IT
- Transformer type: open
- Coil former: horizontal type, 7+7 pins
- Max. temp. rise: 45°C
- Max. operating ambient temp.: 60°C
- Mains insulation: compliance with EN60950.

## 8.1 Electrical characteristics

- Converter topology: asymmetrical half-bridge
- Core type: ETD34 - N87 or equivalent
- Operating frequency: 100 kHz
- Primary inductance: 400 µH 10% at 1 kHz - 0.25 V (see *Note 1*)
- Air gap: 2.32 mm on central leg
- Leakage inductance: 10 µH max. at 100 kHz - 0.25 V (see *Note 2*)
- Primary capacitance: 6 pF typ. (see *Note 3*)
- Max. peak primary current: 1.93 $A_{pk}$
- RMS primary current: 0.75 $A_{RMS}$

*Note: 1 measured between pins 2-4*

*2 measured between pins 2-4 with secondaries and auxiliary windings shorted*

*3 calculated considering primary inductance and resonance frequency*

**Figure 30. Electrical diagram**

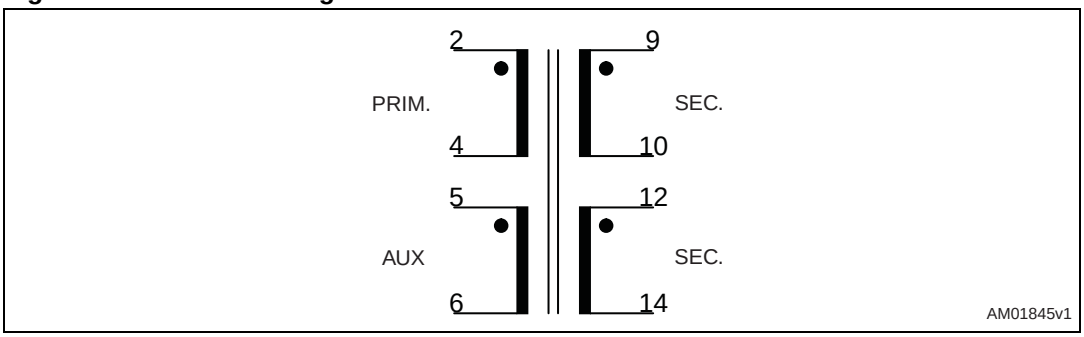

**Table 10. Winding characteristics**

| Pins | Winding | RMS current | Nr. of turns | Wire type |
|---|---|---|---|---|
| 2 – 3 | Primary A | 0.75 $A_{RMS}$ | 35 | Ø 0.355 mm – G2 |
| 9 – 10 | Secondary 1 | 3.81 $A_{RMS}$ | 4 | Stranded 90 x Ø 0.1 mm – G1 |
| 12 – 14 | Secondary 2 | 6.57 $A_{RMS}$ | 7 | Stranded 135 x Ø 0.1 mm – G1 |
| 3 – 4 | Primary B | 0.75 $A_{RMS}$ | 35 | Ø 0.355 mm – G2 |
| 5 – 6 | Auxiliary | 0.05 $A_{RMS}$ | 3 spaced | Ø 0.355 mm – G2 |

*Note: Primaries A and B are in series*

*Cover wires ends with silicon sleeve*

**Figure 31. Windings position**

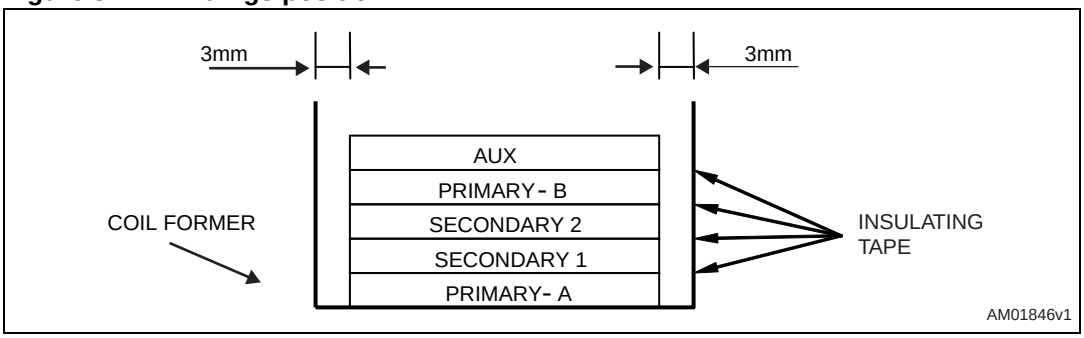


## 8.2 Mechanical aspect and pin numbering

- Maximum height from PCB: 30 mm
- Coil former type: vertical, low profile, 7+7 pins, NORWE ETD34lr/h14/-1/rtg
- Pin distance: 5.08 mm
- Row distance: 25.4 mm
- Pin removed: # 7
- Manufacturer: Magnetica
- P/N: 1754.0004

**Figure 32. Top view**

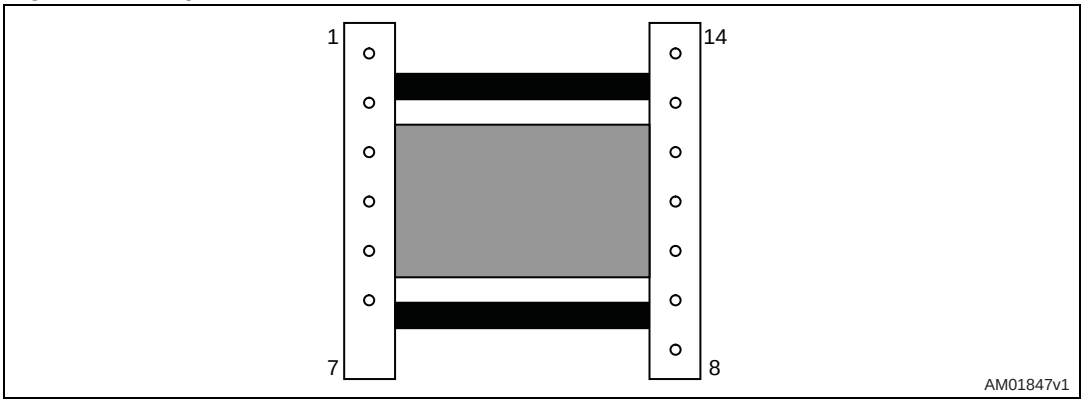

# 9 PCB layout

**Figure 33. Topside silk screen**

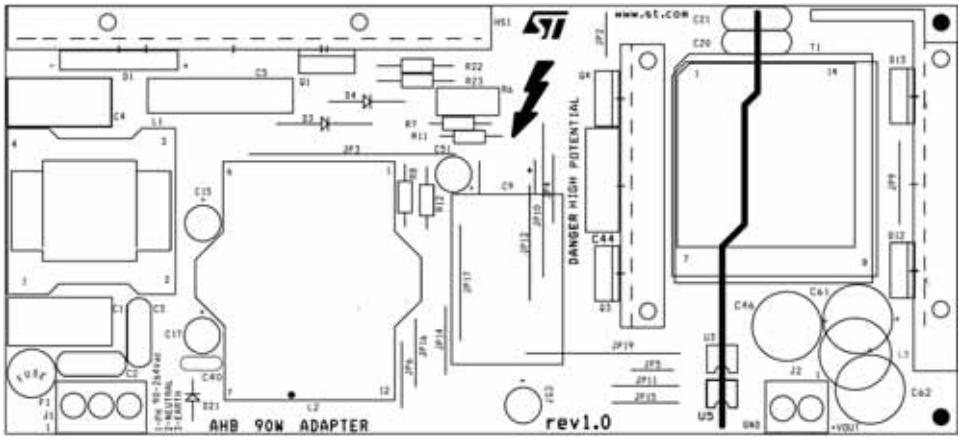


**Figure 34. Bottomside silk screen**

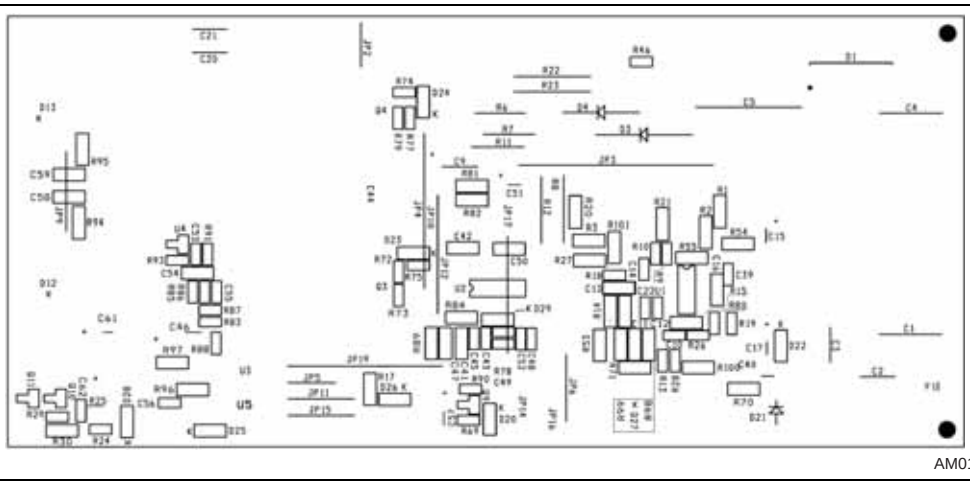


**Figure 35. Copper traces (bottomside)**

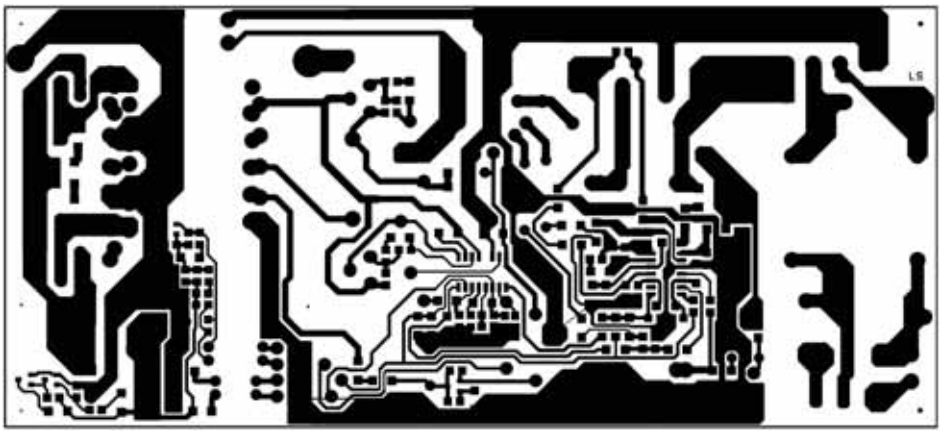

# 10 Revision history

**Table 11. Document revision history**

| Date | Revision | Changes |
|---|---|---|
| 28-Jan-2009 | 1 | Initial release |